# *Chapter-5*

**Synthesis and Characterization of Ti-Nb-Fe alloy- S53P4 Bioactive glass Composite**

## 5.1 Introduction

The growing population and fast running life increase the risk of accidents and critical bone fractures in normal daily life so there is high demand of orthopedic load bearing implant for the hard tissue replacement. These loads bearing implant must be biocompatible and should have matched mechanical properties to that of the cortical and cancellous bones. So a new low modulus Ti alloy, containing nontoxic elements along with high strength and hardness is desirable to replace the current Ti-6Al-4V alloy implant.

The phase diagram of Ti indicates that it has two major phases of importance, namely alpha and beta. Earlier work suggests that Ti containing beta phase possess low Young's modulus as compared to alpha phase [1-12]. The number of beta stabilising alloying elements like Mo, Nb, Fe, Sn, Zr and Ta had been mixed with Ti to produce various alloys such as Ti-Mo [13], Ti-29Nb-13Ta-4.6Zr [14,15], Ti-24Nb-4Zr-7.9Sn [16] and Ti-10Zr-15Nb[17,18] Ti-Nb, Ti –Fe [19,20].

Niobium and iron are the nontoxic elements which stabilize the beta phase in Titanium alloys. Refractory metal *Nb has been studied and* is known to have excellent corrosion resistance and good biocompatibility, viable for their use as biomaterials2,3. Matsuno et al. [8], an in vivo animal study showed that healing around the position where the metallic wires were inserted in the animal (near to soft and hard tissues) proceed rapidly. Moreover, the experiments showed the formation of new bone well attached to the surface of the

metal implant, i.e., the metals have good biocompatibility and osteoinductivity. Some other reports about the biological response of the cells in contact with Nb came from the evaluation of TiNbx alloys, in which Nb had been introduced to substitute Al or V [9–12]. In all cases it was demonstrated that the short and long-term biocompatibility of Nb was excellent; it was a good alloying substitute providing the mechanical strength to the Ti alloys, as well as a biocompatible element. In vitro and in vivo studies indicate that Nb (TiNb), in contrast to (TiNi), was cytocompatible and hypoallergenic [13]. In addition to better biocompatibility and resistance to corrosion, Ti-Nb alloys exhibit a very low value of Young's modulus combined with good mechanical strength depending on composition and phase transformation [21, 22]. Fe is low-cost material and positively affects the osteogenesis as well as other functional mechanisms in the body. The addition of Fe in Ti-Nb alloys changes its beta phase stability thereby balances both the phases [23, 24].

The difficulties in Ti processing arise due to the contamination and good reactivity at high temperature. So the powder metallurgy (PM) method is adopted for the processing. The elemental powders are mixed by high energy ball milling, where the collisions occur within the tungsten ball used. This also raises the span of solubility of the solid in the alloy.

Bio-active glasses are the novel bioactive materials which are generally based on silicate, borate, and phosphate assembly. [29].These are different from conventional glass in terms of bioactivity. The first bioactive glass 45S5 was invented by Hench, which is based on a silicate structure and contains calcium and phosphate. It exhibits excellent bonding properties with the tissues and also boosts the bone growth [30-31]. The degradation rate of these silicate glasses are slow due to $SiO_2$ layer formation inside the human body.S53P4

is another silica-based bioactive glass with the weight percent composition 53 % SiO2, 20 % Cao, 23%Na2O, and 4 % P2O5. It also exhibit noble bioactivity in the cells. However, the low strength and brittleness of the glass restricted its application in the soft tissues [32, 33].

In this work, comparatively, cost-effective Ti-8Nb-2Fe alloy is synthesized with the help of powder metallurgy. The synthesized alloy is mixed with S53P4 bioactive (BAG) glass in the range of 0 - 20%. BAG S53P4 is selected due to its ability to degrade the human body environment and transform into hydroxyl-apatite. The main goal of current work is to combine the physio-mechanical properties of Ti alloy matrix with the biological properties of S53P4 glass and to eliminate the disadvantage of the coating by mixing the glass within the alloy matrix in place of coating.

## 5. 2. Experimental

### 5.2.1 Raw Material Used

In this study, pure titanium (98%), Niobium(99%), and Iron(98%) powders are used for the alloy powder preparation. Bioactive glass is synthesized by using AR grade Quartz (99% SiO2), Calcium Carbonate (99%CaCO3), and, Sodium Carbonate (99%Na2CO3),NaCl, NaHCO3, KCl, K2HPO4 3H2O, MgCl2 6H2O, CaCl2, and Na2SO4tris((CH2OH) 3CNH2) and 1 M HCl is used to prepare (SBF) simulated body fluid.

### 5.2.2 Alloy synthesis

The powder of Ti is mixed mechanically with 8 wt% of Niobium (Nb) and 2 wt% of Iron (Fe) powders in a planetary mill. Steel jar and tungsten balls have been used as a mixing media for the production of alloy. The powder-to-ball weight ratio has been taken as 8:1. The milling has been performed in an argon atmosphere to prevent it from oxidation.

The milling is carried out up to 7 h for the mixing of alloy powder. Due to the malleable property of metal powders; some quantity of process control agent,(PCA) i.e. three weight % ethanol was added during the milling operation. The PCA refreshes the contacts of metal surfaces and minimizes the welding of the powders otherwise it may cause oxidation and contamination [34].

### 5.2.3 Glass Preparation

The batch having components 53 % $SiO_2$, 20 % Cao, 23%$Na_2O$, 4 % $P_2O_5$, as weight percentage were weighed. The raw materials areSilica (99% $SiO_2$ ), Calcium Carbonate (99%$CaCO_3$), Sodium Carbonate (99%$Na_2CO_3$) and Di Sodium Hydrogen Phosphate. The material was mixed for 20 minutes in an agatemortar. These reagents in a platinum crucible were heated for 5 h in a furnace at 14500C. Then the melt has been quenched in water and milled to bring finally the form of powder.

### 5.2.4 Composite preparation

The crushed powder of S53P4BAG has been mixed in the matrix of prepared alloy powder in the weight percentage of 5, 10, and 20 respectively (Table 1) and milled for 30 minutes

to obtain a homogeneous mixture and the binder 0.4 % of dextrin is also added in the mixture. The bar and pallets of these composite powder were fabricated with the help of a uniaxial press machine by applying the pressure of 470 MPa. The sintering of these samples was done in two steps. Firstly the samples were sintered at 6500C for 1 h to remove the dextrin. Then it was further heated in a high temperature control atmosphere furnace with the dwell time of 4.5 h at 1300 °C at the heating rate of 10 °C/min. The rate of cooling has been kept initially at 15 °C/min until the temperature reaches 870°C and then with faster rate30°C/min.

**Table .5.1 Composition of Ti-8Nb-2Fe –BAG Composite in weight %**

| Sample | N1 | N2 | N3 | N4 |
|---|---|---|---|---|
| Alloy (Ti-8Nb-2Fe) | 100 | 95 | 90 | 80 |
| BAG (S53P4 ) | 00 | 05 | 10 | 20 |

### 5.2.5. Characterization

The portable powder XRD machine (Rigaku, Japan) using copper Kα radiation has identified the major phases in the prepared samples. The phases have been identified by matching the respective XRD peaks with that of JCPDS database.

For the microstructure examination, all prepared composites have been polished by emery papers of various grades. The samples were kept in a Kroll solution: 3 ml HF, 6 ml HNO3, 100 ml H2O and micrograph (SEM) have been taken using INSPECT 50 FEI.

Compressive strength measurement was performed with the UTM with a strain rate of 2.0 mm/min. Elastic moduli were measured with the help of ultrasonic gauge (45MG, Olympus, USA), by calculating sample density. The transverse velocity and longitudinal velocity have been measured by ultrasonic technique. The indentation method has been performed for the hardness of the samples with the help of Vickers's hardness with the force of 2 kgf, and depression of the mark has been noted through the microscope.While performing mechanical characterizations, five samples for every group (N1, N2, N3 and N4) were taken. The mean value and standard deviation have been determined and the results are presented as a mean value ± standard deviation within permissible error bars.

The apparent porosity and bulk density are measured by Archimedes method due to its authenticity and simplicity. Initially, the dry weight of sample have been measured then all samples have been suspended in water by using steel wire and suspended, and soaked weight was determined and the bellow mathematical equations are used for the calculating the density and apparent porosity [35].

Apparent porosity (A.P %) = X 100, Where W=suspended weight in gm

Bulk Density (B.D gm/cm3) = S= Soaked weight in gm

D=Dry weight in gm

The bioactive analysis is carried out by immersing all the samples in simulated body fluid (SBF) for some days. The preparation of SBF has been done by using NaCl, KCl, NaHCO3, MgCl2•6H2O, CaCl2, and KH2PO4 in doubled distilled water. The prepared SBF possesses similar concentrations of ions as found in human body fluid. In the beaker; the samples to be tested were dipped in simulated body fluid and kept for 7 days at 37 °C. The pH of simulated body fluid was observed continuously for 7 days. After immersion, the samples were again dried for 15 minutes, and their SEM analysis was done.

The weight loss method was used for the corrosion analysis of the samples. The composites have been immersed in simulated body fluid at 370C for several days. Firstly, the dry weight of the samples has been measured, and after immersion, the samples were weed out from simulated body fluid at the regular interval for wet weight measurement. Then the samples were cleaned with the water for the removal of any corrosion by-products, the corrosion rate is determined by using the following formula [37].

Corrosion Rate (millimetre/year) =

Where A= Area of samples in cm2

D= Density of the sample in g/cm3.

W =weight loss in mg

T=Time of immersion in hours

In-vitro cellular response of Ti alloy and composites in the present study were performed for human osteosarcoma, SaOS2 cells. The cell lines were purchased from NCCS Pune, India. The received cells were firstly grown with complete media, which consists of McCoy' 5A, 15% fetal broken serum (FBS) and 1% antibiotics at 37 oC in a CO2 incubator. The autoclaved samples were seeded with 10,000 cells per well for 3, 5, and 7, days. The MTT [3-(4,5-dimethylthiazol-2-yl)-2,5-diphenyltetrazolium bromide] assay of seeded samples were performed after the respective incubation period. The samples were cleaned with 1x PBS and further incubated with MTT (MTT: Media in the ratio of 1: 10) for 6 hrs. MTT reads with cells and forms purple color formazan crystal, which can be dissolved in DMSO (dimethyl sulfoxide). The absorbance of dissolved crystal was determined using Elisa micro plate reader at 595 nm. The viability is calculated as follows [38]

The statistical analysis of optical density was performed by one way ANOVA followed by Tukey'spost hoc test for comparison of respective result. Each experiment was performed in triplicate and significant differences have been considered for ‘p’ value <0.05.

### 5.2.6. Result and Discussion

#### 5.2.6.1 Phase Analysis

The XRD patterns of prepared samples are shown in figure 5.1.XRD of pure alloy N1 contains dual phase alpha and beta titanium. The X-ray pattern reveals that metal alloy without bioactive glass (N1) has hexagonal α Ti (PCPDF No 892762) as a major phase with some sort of BCC β Ti (PCPDF No-894913). In addition to alpha and beta titanium,

the brittle intermetallic compound Ti4Nb (PCPDF No 657479) and TiFe (PCPDF No 655613) also formed. With the reinforcement of S53P4bioactive glass in Ti alloy matrix (N2, N3 & N4), some additional peaks of TiP (PCPDF No.731821), Na2CaSi3O8 (PCPDF No.120671) are also observed in the pattern as a reaction between metal and glass constituents. XRD pattern of composite suggests that the intensity of these peaks increases with the weight percentage of reinforced BAG.

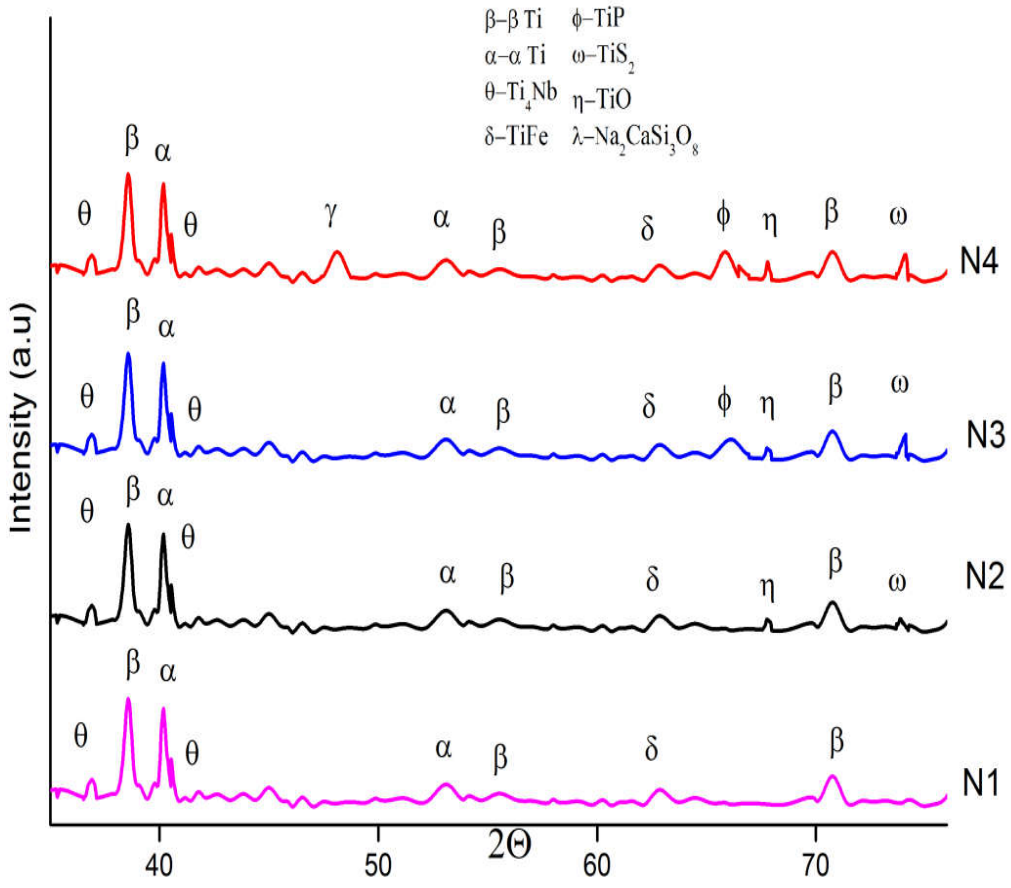


**Fig.5.1 XRD spectra of synthesized composites**

### 5.2.6.2 Scanning Electron Microscopy (SEM)

The scanning electron micrographs of samples are represented in figure 2. The pure alloy contains a dual phase structure having alpha and retained beta phase as depicted in fig 2(a, b). The smaller amount of glassy phase appears on the surface of samples in fig 2 (c, d) with negligible pores where the reinforced glass is 5 %.On increasing volume percentage of BAG to 10 % and 20 %, the surface becomes more glassy with increased porosity as shown in micrograph 2(e, f, g, h). During sintering,some amount of bioactive glass melted which distributed uniformly on surface of the alloy. The flatter glassiness phase ensures the uniform distribution of bioactive glass on the surface.

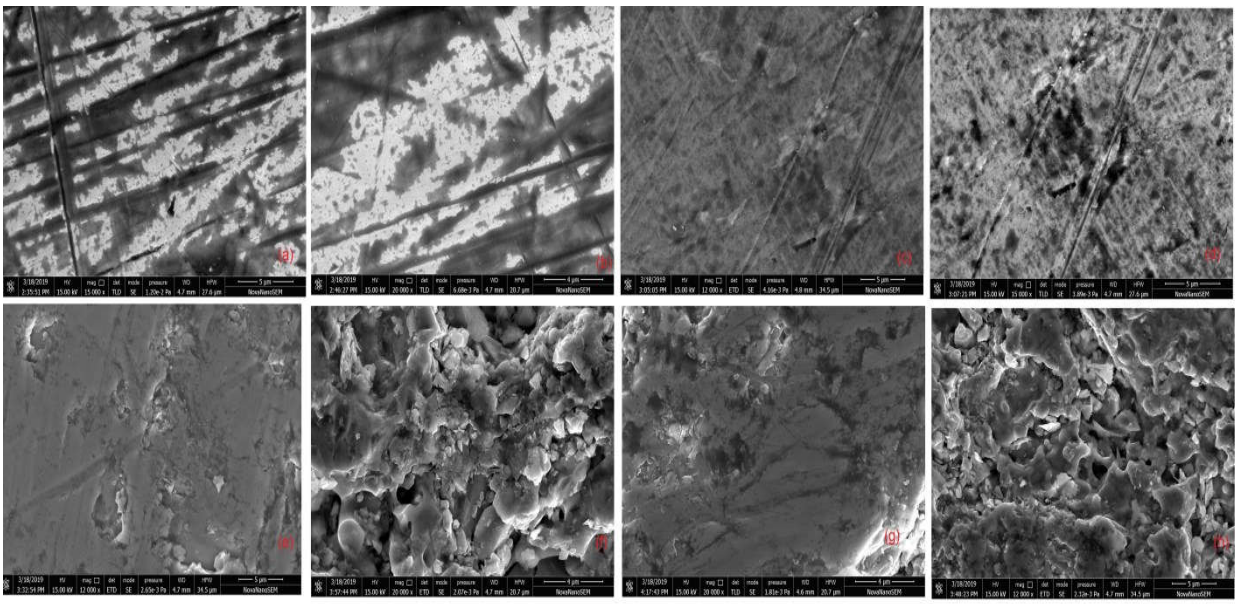

**Fig.5.2 Scanning Electron Micrographs of alloy N1(a,b),Alloy + 5%BAG N2(c,d) Alloy +10%BAG N3(e,f) Alloy + 20%BAG N4(g,h)**

### 5.2.6.3 Physio-mechanical properties

Figure 5.3 (a) and 5.(b) illustrate the bulk density and apparent porosity of the samples. From the graph it is clear that pure alloy sample N1 exhibit the bulk density and apparent porosity of 4.55 gm/cm3 and 3.9% respectively. As we increases the reinforced percentage of S53P4 bioactive glass in the matrix, the apparent porosity of the sample N2, N3 and N4 increases whereas the density decreases. This is due to the fact that, with increased volume fraction of bioactive glass, the internal friction between glass particles and matrix increases which obstruct the solidification resulting in increased porosity [39,40].

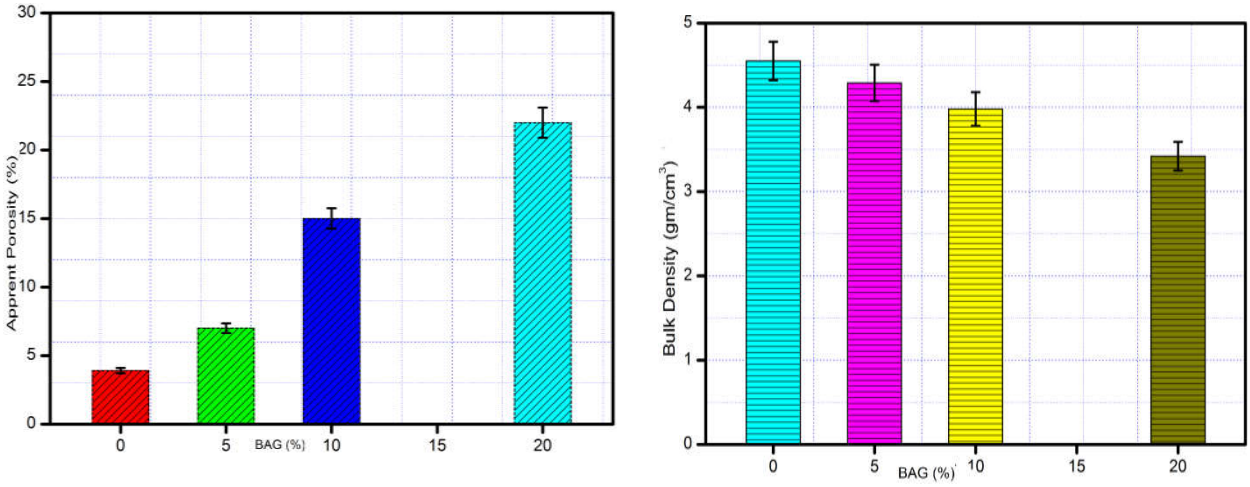


**Fig. 5.3 (a) Bulk Density of the prepared samples 5.3 (b) Apparent Porosity of the prepared samples**

The Vickers's hardness of samples are shown in fig 5.4.The pure alloy matrix N1 shows the increased hardness value of 507 Hv as compared to pre-existing Ti-6Al-4V alloy. This enhanced value of hardness is due to the Ti-Fe and Ti4Nb intermetallic formed between

the metallic powders. The Hardness of the composites, N2, N3 and N4 shows the value of 542 Hv, 522, and 510 Hv respectively.

It is obvious from the graph that, when the reinforced percentage of BAG is low (5%),the hardness increases to 542 Hv , but as the reinforced phase increases to 10% and 20% ,the value of hardness reduces to 522 and 510 Hv respectively. These values of hardness are greater than that of reported values of Ti-6Al-4V alloys as well as cortical bone [41].The clarification to this behaviour is that when BAG is in low percentage in the matrix, the porosity affects by little amount and the hardness increases due to work hardening and some new phases (Tio, TiP) formed in the composite [42]. But with the increased volume percentage of BAG, considerable amount of porosity is induced as indicated in fig 3(b) which further reduces the hardness of the composite.

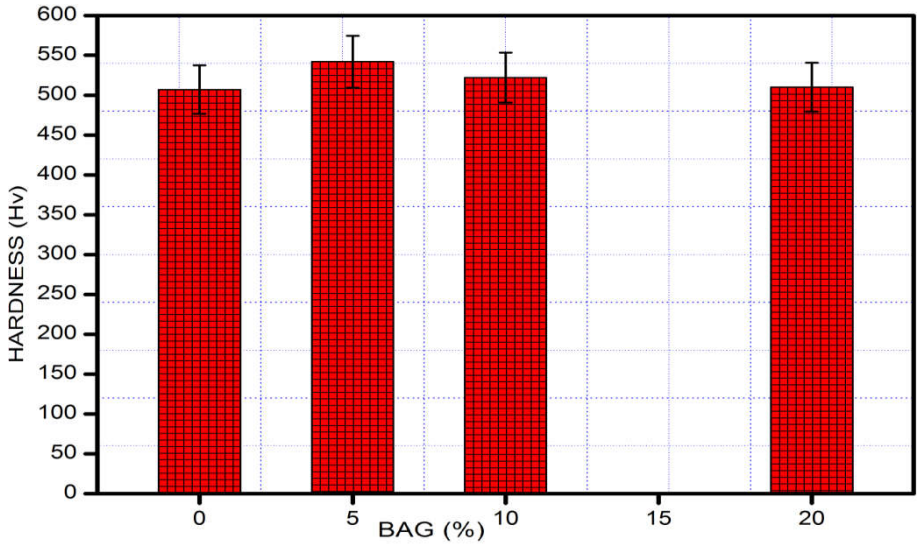


**Fig. 5.4 Vickers's hardness of all the samples**

The compressive strength for the samples N1,N2,N3, and N4 are represented in fig 5. The graph indicated that the alloy N1 exhibit the compressive strength of 521 MPa, whereas

the reinforced samples N2, N3, and N4 shows the value of 610 MPa,585 MPa and 542 MPa respectively which are still greater than the cortical bone. From the figure, it is also clear that the strength of composites increased first with the reinforcing BAG concerning N1 and then decreases when the volume fraction of BAG further increases to 10% and 20%.

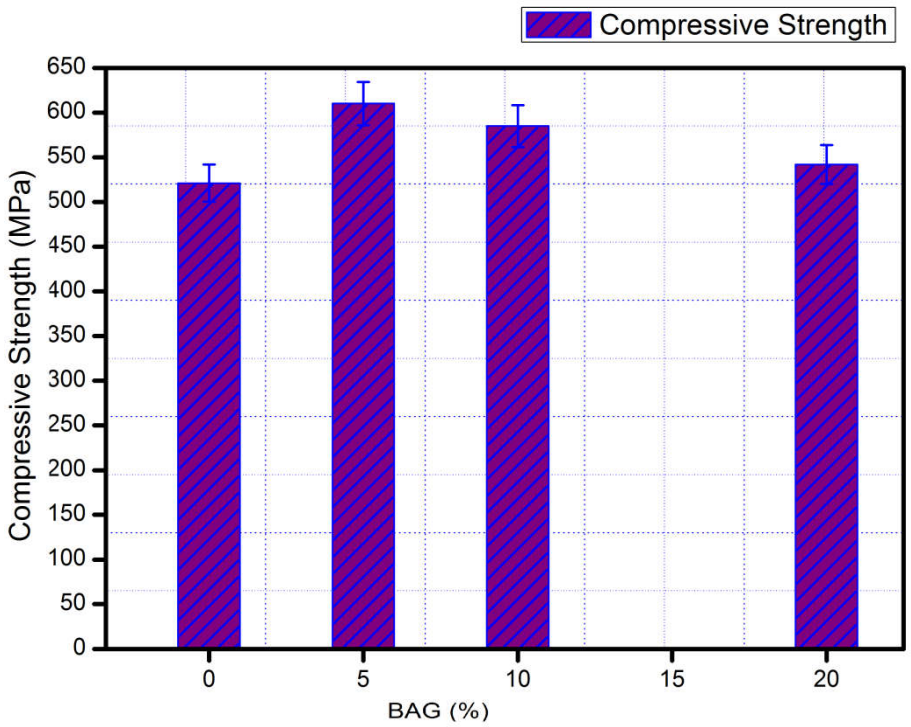


Fig. 5.5 Compressive Strength of the samples N1, N2, N3 & N4

Fig 5.6 shows the elastic modulus of the prepared samples measured from the ultrasonic gauge. The modulus of alloy sample N1 without reinforcing phase exhibit the value of 92 GPa and decreases in the composites N2 (81 GPa), N3 (72 GPa) and N4 (63 GPa) as the

reinforced percentage of S53P4 BAG increases. This reduced value of elastic modulus is useful to reduce the stress shielding effect in the implant [43].

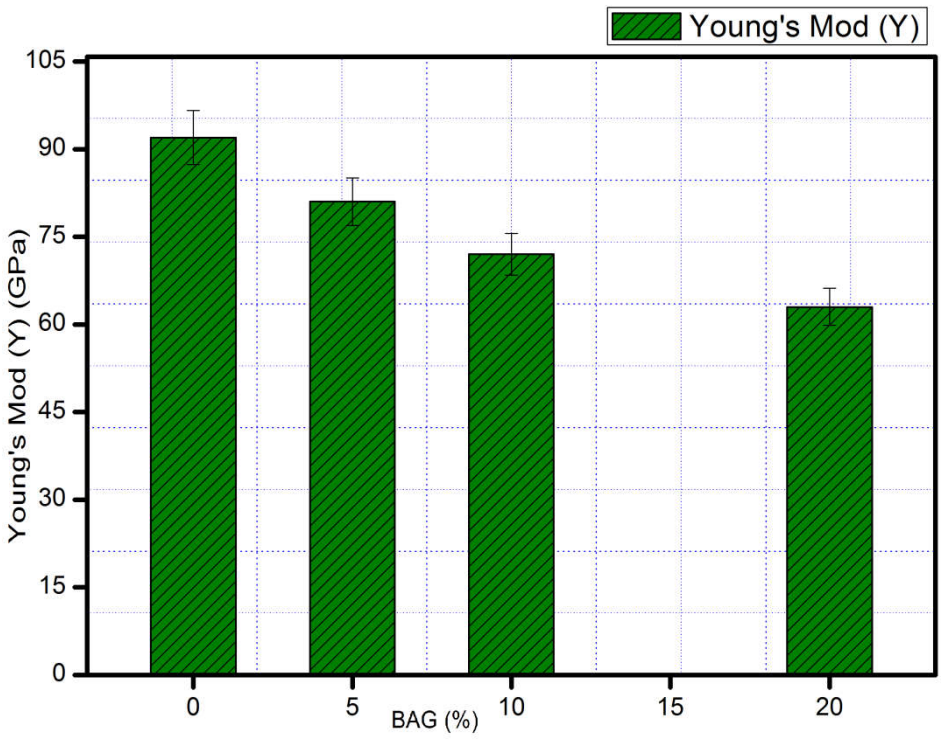


**Fig. 5.6 Elastic Mod of all the prepared samples**

### 5.2.6.4 In vitro Bioactivity

To analyze the in vitro bioactivity, the samples were immersed in SBF solution, and pH behavior of the solution was observed at different immersion time up to seven days. Fig

5.7 shows the change in pH of the SBF solution after immersing the samples. From this graph, it is clear that the pH of all the composite having BAG increases rapidly as compared to pure alloy matrix N1. The graph also depicts the pH value and its rate of change increase with the increased amount of reinforced bioactive glass. The H+ ions in SBF solution are being replaced by network modifier cations (Na +, Ca+) released by the surface of the samples which cause an increase in hydroxyl concentration of the solution thereby increases the pH of the SBF solution[43].

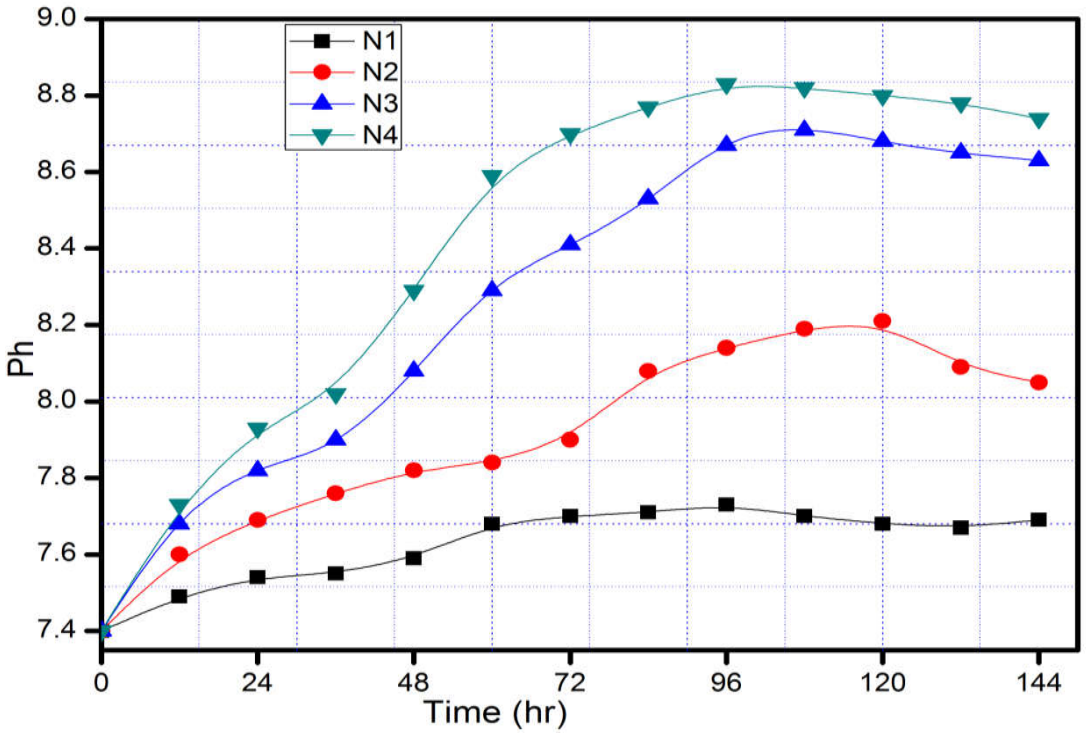


**Fig. 5.7 In vitro pH behavior of the samples in SBF**

The cat-ions released from the bioactive glass when coupled with the phosphate ions of simulated body fluid lead to the construction of the hydroxyl appetite layer on the surface of the composite. The SEM micrographs have also been taken after seven-day immersion

of the samples to confirm this fact. Fig 5.8 shows the change in the morphology of the surface when it is compared to the primary stage of composites before immersion (fig5.2)

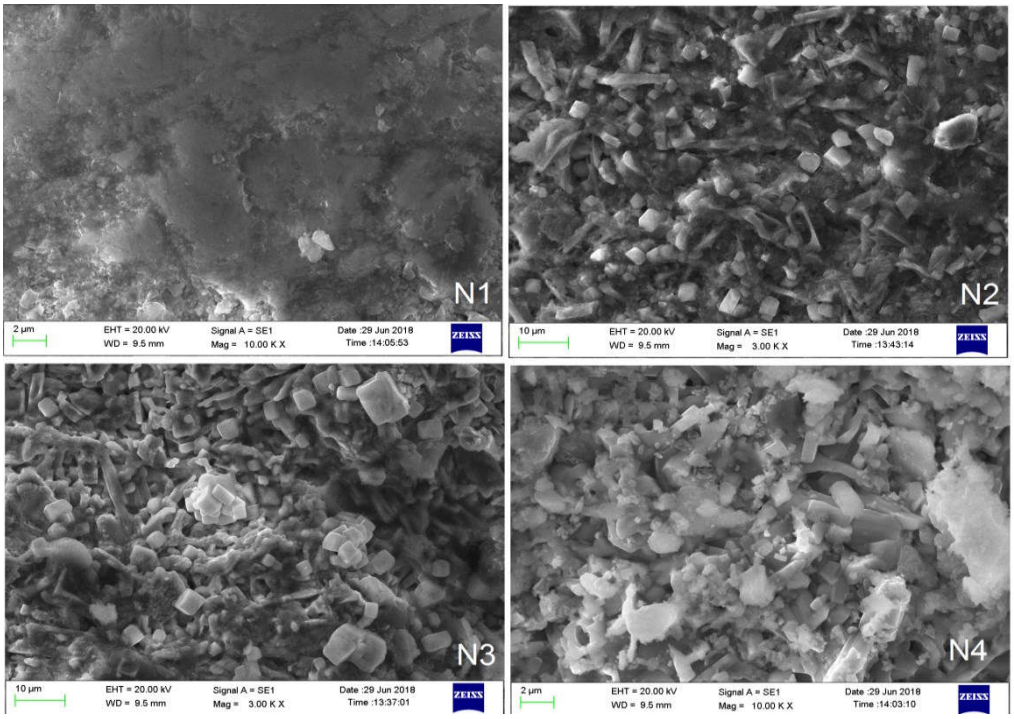


**Fig. 5.8 SEM Micrographs of all the samples after immersion in SBF**

### 5.2.6.5 Corrosion Study

The effect of SBF solution on the corrosion rate of composites has been studied by weight loss method. Fig 5.9 shows the corrosion rate of composites concerning the immersion time. The graph predicts that the pure alloy sample N1 exhibit the corrosion rate of .0082 millimeter per year (mmpy) after 42 days of immersion. Initially, the high corrosion rate of composites N2, N3 and N4 having S53P4 bioactive as compared to N1 are due to the reason that in the beginning, the degradation of S53P4 bioactive glass occurs rapidly until the HCA layer is formed on the surface of the composite. The HCA layer ceases the further degradation of BAG hence the weight loss and so rate of corrosion of N2, N3, and N4 approximately reaches nearly equal to the pure alloy sample N1.

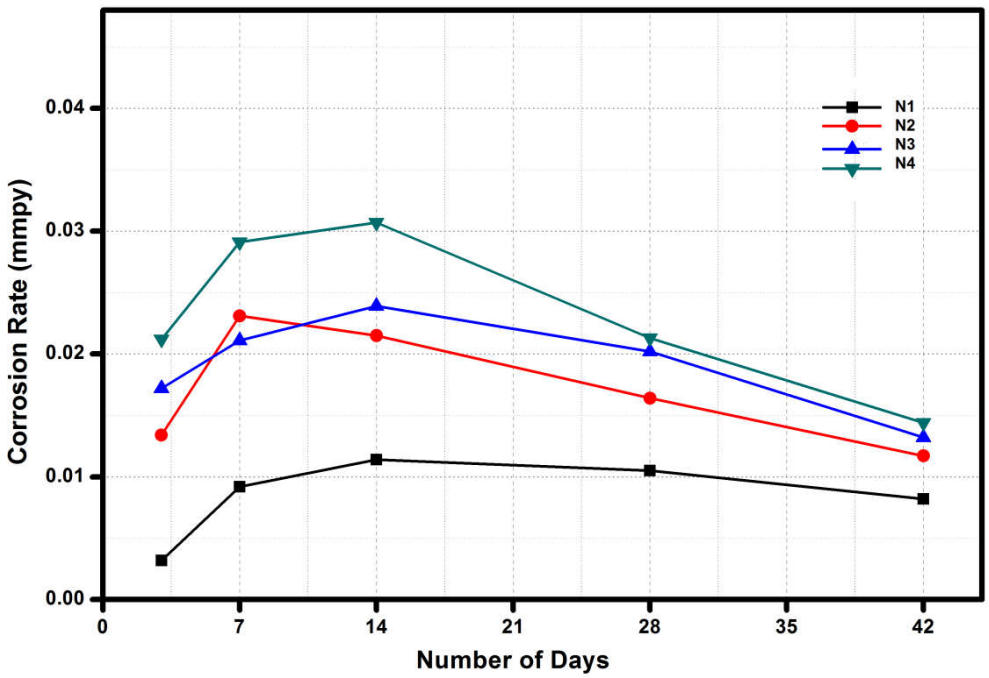


**Fig. 5.9 Rate of corrosion of alloy (N1) and composites having BAG (N2, N3, N4)**

### 5.2.6.1 Cell Culture Study

Fig. 5.10 represents the viability of SaOS2 cells seeded on Ti alloy and composites. It is observed from fig. All samples shows a significant difference concerning control (*) after 3,5 and seven days. From the figure 10, it is also clear that reinforcement of bioactive glass significantly increases the viability of SaOS2 cells as compared to pure alloy matrix N1 (**) and the viability of N1 sample has no significance increment after 5 and seven days. However, on the other hand, N2, N3 and N4 samples show higher viability after 5th and 7th days.

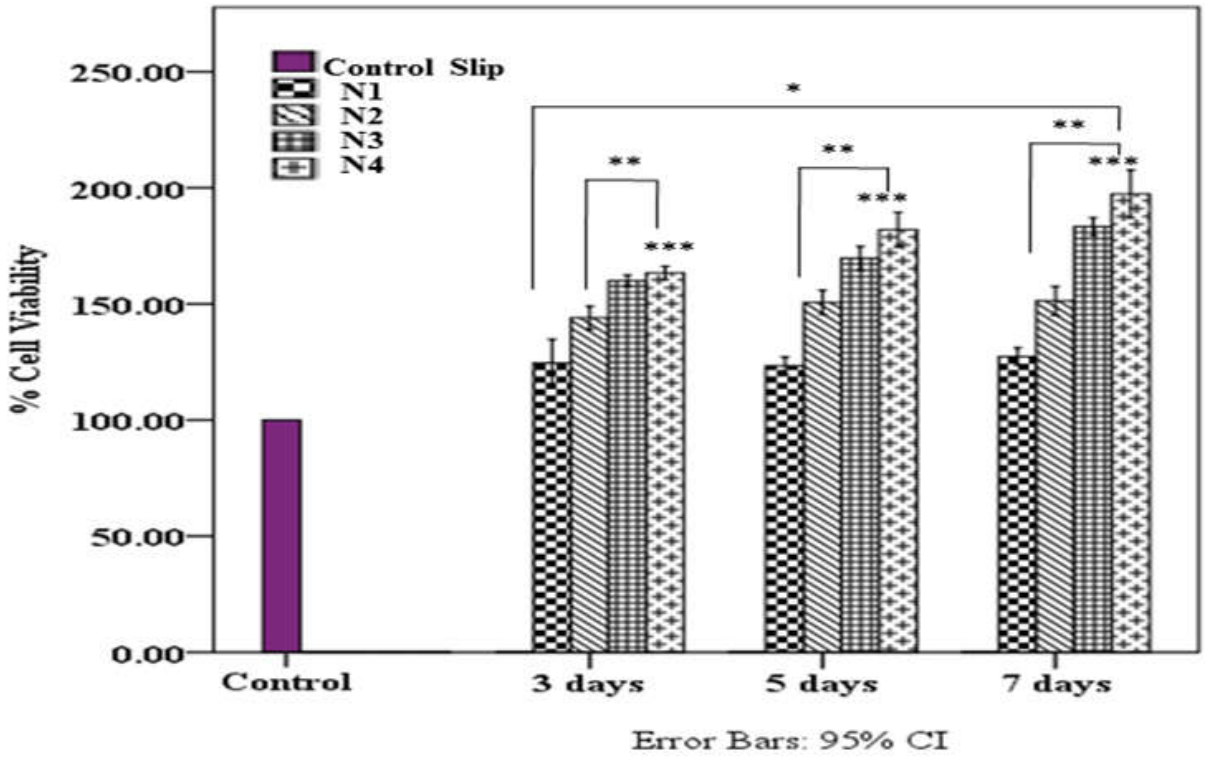


**Fig. 5.10 Time-dependent Viability of SaOS2cells in all the prepared samples (N1, N2, N3, & N4)**

## 5. Conclusion

The effect of S53P4 bioactive glass addition on the physio-mechanical, biological, and corrosion properties of newly developed composite for the orthopedic implant was examined and subjected to the following results.

1.The porosity of prepared samples increases on increasing the volume fraction of the reinforced bioactive glass and shows the value of 7% (N2), 15% (N3) and 22 %( N4) due to increased frictional mechanism between the metal matrix and glass particle.

2.Pure Ti-8Nb-2Fe shows the compressive strength of 521 MPa while composite N2,N3 & N4 exhibit the compressive strength of 610,585 and 542 MPa which are superior to cortical bone.

3.Due to the formation of intermetallic and intermediate compounds, the Hardness of pure alloy N1 as well as reinforced composite N2, N3 and N4 increases as compared to Ti-6Al-4V alloy and attains the value of 507,542,522 and 510 Hv respectively which are greater than the cortical bone also.

4.Reinforcement of bioactive glass significantly reduces the elastic modulus of the composite and approaches the value of 81, 72 and 63 GPa in the N2, N3 and N4 samples which comes very close to that of cortical bones and will reduce the stress shielding effect.

5.The formation of hydroxyl appetite layer in SBF in N3 and N4 composite have been observed prominent where the reinforcement percentage reaches 10% and 20% respectively.

6.The cell culture suggests that in all the composites, the bioactivity increases with the reinforced percentage of bioactive glass; however, the composite N4 is found to have maximum bioactivity.

The above result suggests that the composite N4 having 20% reinforcement of S53P4 bioactive glass comes out to be the best composition as it exhibits good biocompatibility, lowest elastic modulus (63 GPa), optimum compressive strength (542 MPa), enhanced bioactivity and increased hardness (510 Hv). So it can be a new potential candidate for orthopedic implant, which can potentially reduce the problem of stress shielding and toxicity.

**References:**

[1] Qizhi Chen George A. Thomas, Metallic implant biomaterials. Materials Science and Engineering: R: Reports. 87(2015)1-57

[2] Mahmoud Z. Ibrahim, Ahmed A.D et.all, biomedical materials and techniques to improve the tribological, mechanical and biomedical properties of orthopedic implants – A review article, Journal of Alloys and Compounds714 (2017) 636-667

[3] LenkaKunčická, Radakovich, Terry C. Lowe, Advances in metals and alloys for joint replacement. Progress in Materials Science 88 (2017) 230-280.

[4] C. Cases, Implant biomaterials: A comprehensive review World Journal of Clinical Cases. 3 (2015) 52-57

[5].Sennerby L, Thomsen P, et al. A morphometric and biomechanic comparison of titanium implants inserted in rabbit cortical and cancellous bone. The International Journal of Oral& Maxillofacial Implants.7 (1992) 62–71.

[6] Walker PR, LeBlanc J, Sikorska M, Effects of aluminum and other cations on the structure of brain and liver chromatin. Biochemistry. 28 (1989) 3911–3915.

[7] Rao S, Ushida T, et al. Effect of Ti, Al, and V ions on the relative growth rate of fibroblasts (L929) and osteoblasts (MC3T3-E1) cells. Bio-Medical Materials and Engineering. 6 (1996) 79–86.

[8] Gomes CC, Moreira LM, et al. Assessment of the genetic risks of a metallic alloy used in medical implants. Genetics and Molecular Biology 34 (2011) 116-121.

[9] G.S. Leventhal, TITANIUM, A METAL FOR SURGERY, J. Bone Joint Surg. 33 (2006) 473–474.

[10]C. Leyens and M. Peter, Titanium and Titanium alloys-fundamental & applications. 09 (2003) 65

[11] GerdLütjering, James C. WilliamsTitanium 2nd ed;2007: Springer Berlin Heidelberg New York

[12] I. J. Polmear, Light Alloys (From Traditional Alloys to Nanocrystals) 4th ed;2006: Butterworth-Heinemann Elsevier, UK

[13] Ho WF, A comparison of tensile properties and corrosion behavior of cast Ti – 7. 5Mo with c. p. Ti, Ti – 15Mo and Ti – 6Al – 4V alloys.J of Alloys and compounds 464 (2008) 580–583.

[14] T. Homma, A. Arafah et al. Effect of alloying elements on microstructural evolution in oxygen content controlled Ti-29Nb-13Ta-4.6Zr (wt. %) alloys for biomedical applications during aging, Materials Science and Engineering: A7093 (2018)12-321

[15]Yoon-Seok Lee, MitsuoNiinomi, et.alWear transition of solid-solution-strengthened Ti–29Nb–13Ta–4.6Zr alloys by interstitial oxygen for biomedical applications, Journal of the Mechanical Behaviour of Biomedical Materials. 51 (2015) 398-408

[16] ShiboGuo, Aimin Chu, Haijiang Wu, Chun Cai, XuanhuiQu, Effect of sintering processing on microstructure, mechanical properties and corrosion resistance of Ti–24Nb–4Zr–7.9Sn alloy for biomedical applications, Journal of Alloys and Compounds.597 (2014) 211-216

[17]Weimin Chen, Interdiffusion and atomic mobility in bcc Ti-rich Ti–Nb–Zrsystem, Calphad. 60 (2018) 98-105

[18] V.Yu. Zadorozhnyy, S.N. Klyamkin, Mechanical alloying of nanocrystalline intermetallic compound TiFe, Journal of Alloys and Compounds 586 (2014) S56–S60

[19] Dmitri V. Louzguine, Hidemi Kato, Akihisa InoueHigh strength and ductile binary Ti–Fe composite alloy, Journal of Alloys and Compounds 384 (2004 )L1–L3

[20] ShimaEhtemam-Haghighi, Yujing Liu et al. Phase transition, microstructural evolution and mechanical properties of Ti-Nb-Fe alloys induced by Fe addition, Materials and Design 97 (2016) 279–286

[21] Hsueh-ChuanHsua, Shih-Kuang structure and mechanical properties of as-cast Ti–5Nb–xFe alloys Materials Characterization 61 (2010) 851-858

[22] Camilo A.F. Salvador, Mariana R. Dal BóSolute lean Ti-Nb-Fe alloys: An exploratory study, Journal of the mechanical behavior of biomedical materials 65 (2017)761–769.

[23] Hideki Hosoda1, a Kenta Kasuya, Mechanical Properties of Ti-Fe-Sn Biomedical Alloys with or without Aging TreatmenMaterials Science Forum. 786 (2014) 2423-2428

[24] Arne Biesiekierski, Jixing Lin, Investigations into Ti–(Nb, Ta)–Fe alloys for biomedical applications, ActaBiomaterialia. 32 (2016) 336-347

[25] Li Y, Lee I, et al. The biocompatibility of nanostructured calcium phosphate coated on micro-arc oxidized titanium. Biomaterials. 29 (2008) 2025–2032.

[26] SilviaSprianoa, Seiji Yamaguchi et al. A critical review of multifunctional titanium surfaces: New frontiers for improving osseointegration and host response, avoiding bacteria contamination. ActaBiomaterialia. 79 (2018) 1-22.

[27] Yang CY, Chang E, Bond degradation at the plasma sprayed HA coating /Ti--6AI-4V alloy interface: an in vitro study, Journal of materials science: materials in medicine. 6 (1995) 258-265.

[28] Julian R. Jones, Alexis G. Clare Bio-Glasses- An Introduction chapter 2, (2012) John Wiley and Sons, Ltd. Willey

[29] Tripathi H, Rath C, et al. Structural, physicomechanical and in-vitro bioactivity studies on SiO2–CaO–P2O5–SrO–Al2O3 bioactive glasses. Materials Science & Engineering C. 94 (2019) 279–290.

[30] Tripathi H, Kumar S, et al. Structural characterization and in vitro bioactivity assessment of SiO 2 – CaO – P 2 O 5 – K 2 O – Al 2 O 3 glass as a bioactive ceramic material. Ceramics International 41 (2015) 11756–11769.

[31] Tripathi H, Kumar AS, et al. Preparation and characterization of Li2O – CaO – Al2O 3 – P2O5 – SiO2 glasses as bioactive material. Bull. Mater. Sci. 39 (2016) 365–376.

[32] N. A. P. van Gestel,1 J. Geurts, Clinical Applications of S53P4 Bioactive Glass in Bone Healing and Osteomyelitis Treatment: A Literature ReviewBioMed Research International .684826 (2015) 12

[33] D.J. Hulsen, N.A. van Gestel,4 - S53P4 bioactive glass management of Periprosthetic Joint Infections (PJIs), Wood head Publishing. (2017) 69-80,

[34] Nouri A, Wen C, Surfactants in Mechanical Alloying / Milling : A Catch-22 Situation Critical Reviews in Solid State and Materials Sciences 39 (2014)81-108.

[35] Loop W, Standard Test Method for Water Absorption, Bulk Density, Apparent Porosity, and Apparent Specific Gravity of Fired White ware Products 88 (2018) 1–2.

[36] Kokubo T, Kushitani H, et al. Solution to reproduce in vivo surface-structure changes in bioactive glass-ceramic A-W3. J of Biomedical Materials Research 24 (1990) 721–734.

[37] Gardner S. Haynes, Laboratory Corrosion Tests and Standards, American Society for Testing and Materials 04 (1985) 529.

[38] Vipul Saxena, Vijay Kumar, Amrendra Raiet.alOptimization of the bio-mechanical properties of Ti–8Si–2Mn alloy by 1393B3 bioactive glass reinforcementMater. Res. Express 6 (2019) 075401

[39] Dai LH, Ling Z, et al. Size-dependent inelastic behavior of particle-reinforced metal - matrix composites. Composites Science and Technology 61 (2001)1057–1063.

[40] Su Y, Ouyang Q, et al. Composite structure modeling and mechanical behavior of particle reinforced metal matrix composites. Materials Science & Engineering A. 597 (2014) 359–369.

[41] Weaver J K, et al. The microscopic hardness of Bone.J Bone Joint Surg 48 A2 (1966) 273-88.

[42] Z. Oksiuta, J.R. Dabrowski a, A. Olszyna, Co–Cr–Mo-based composite reinforced with bioactive glass, Journal of materials processing technology. 209 (2009) 978-985.

[43] Angaraj Singh and Ashutosh Kumar Dubey, Various biomaterials and techniques for improving antibacterial response, ACS Appl. Bio Mater.1(1) (2018) 3–20